

Critical Temperature of Chiral Symmetry Restoration for Quark Matter with a Chiral Chemical Potential

M. Ruggieri

College of Physics, University of Chinese Academy of Sciences, Yuquanlu 19A, Beijing 100049, China.

E-mail: marco.ruggieri@ucas.ac.cn

G. X. Peng

College of Physics, University of Chinese Academy of Sciences, Yuquanlu 19A, Beijing 100049, China.

Theoretical Physics Center for Science Facilities, Institute of High Energy Physics, Beijing 100049, China.

E-mail: gxpeng@ucas.ac.cn

Abstract. In this article we study restoration of chiral symmetry at finite temperature for quark matter with a chiral chemical potential, μ_5 , by means of a nonlocal Nambu-Jona-Lasinio model. This model allows to introduce in the simplest way possible a Euclidean momentum, p_E , dependent quark mass function which decays (neglecting logarithms) as $1/p_E^2$ for large p_E , in agreement with asymptotic behaviour expected in QCD in presence of a nonperturbative quark condensate. We focus on the critical temperature for chiral symmetry restoration in the chiral limit, T_c , versus μ_5 , as well as on the order of the phase transition. We find that T_c increases with μ_5 , and that the transition remains of the second order for the whole range of μ_5 considered.

PACS numbers: 12.38.Aw, 12.38.Mh

Keywords: Chiral chemical potential, nonlocal Nambu-Jona-Lasinio model, chiral phase transition.

1. Introduction

Systems with chirality imbalance, namely with a finite chiral density $n_5 = n_R - n_L$ generated by quantum anomalies, have attracted some interest in recent years. In fact gauge field configurations with a finite winding number, Q_W , can change fermions chirality according to the Adler-Bell-Jackiw anomaly [1, 2]. In the context of Quantum Chromodynamics (QCD) such nontrivial gauge field configurations with $Q_W \neq 0$ are instantons and sphalerons, the latter being produced copiously at high

temperature [3, 4]. The large number of sphaleron transitions in high temperature phase of QCD suggested the possibility to measure the Chiral Magnetic Effect (CME) [5, 6] in heavy ion collisions. The interest for mediums with a net chirality has then spread from QCD to hydrodynamics and condensed matter systems [7, 8, 9, 10, 11, 12, 13, 14, 15, 16, 17, 18, 19, 20, 21, 22].

In order to describe systems with finite chirality in thermodynamical equilibrium, it is customary to introduce the chiral chemical potential, μ_5 , which is conjugated to n_5 , see [23, 24, 25, 26, 27, 28, 29, 30, 31, 32, 33, 34, 35, 36, 37, 38, 39] and references therein. Naming τ the typical time scale in which chirality changing processes take place, it can be assumed that $\mu_5 \neq 0$ describes a system in thermodynamical equilibrium with a fixed value of n_5 on a time scale much larger than τ . For example in the quark-gluon plasma phase of QCD chirality changing processes have been studied in [40] where it has been found that $\tau \simeq 50 \div 140$ fm/c in the temperature range $T \simeq 225 \div 500$ MeV.

An interesting problem in the context of QCD is the study of chiral symmetry restoration at finite temperature and $\mu_5 \neq 0$. Some previous calculations based on chiral models predicted T_c , the critical temperature for chiral symmetry restoration, to decrease with μ_5 [24, 25, 26, 27, 28]. On the other hand, lattice simulations have shown that T_c increases with μ_5 [30, 31], in agreement with the results obtained by solving Schwinger-Dyson equations [34, 35].

In this article we study chiral symmetry restoration at finite temperature with $\mu_5 \neq 0$, within a Nambu-Jona-Lasinio (NJL) model [41, 42, 43, 44, 45] with a nonlocal interaction kernel [46, 47, 48, 49, 50, 51, 52]. The main result of our study is that T_c increases with μ_5 for all the nonlocal kernels used in actual calculations. Moreover, we discuss the order of the chiral phase transition at finite μ_5 : we find that although the chiral chemical potential makes the phase transition sharper, it remains of the second order in the range of μ_5 studied. Both $T_c(\mu_5)$ and the absence of a critical endpoint are in agreement with the most recent lattice results mentioned above.

The plan of the Article is as follows. In Section 2 we briefly describe the nonlocal NJL model we use in our calculation, presenting the several choices we do for the running dependent mass. In Section 3 we compute the critical temperature for chiral symmetry restoration as a function of μ_5 , as well as determine the order of the phase transition. In Section 4 we perform a small μ_5 computation of the second Ginzburg-Landau (GL) coefficient in the free energy. Finally in Section 5 we draw our conclusions.

2. NJL model with momentum dependent quark mass function

In this Section we describe the model we use to compute the critical line for chiral symmetry restoration in the $T - \mu_5$ plane. We use a Nambu-Jona-Lasinio (NJL) model [41, 42] (see [43, 44, 45] for reviews) with a nonlocal interaction kernel inspired by the Instanton Liquid picture of the QCD vacuum [48, 46, 47, 49, 50], see [53] for a review, which has the advantage to introduce in the simplest way possible a Euclidean momentum dependent quark mass function that agrees with QCD [54, 55].

2.1. Thermodynamic potential

In the nonlocal NJL model we use in this study the lagrangian density is given by

$$\mathcal{L} = \bar{\psi} (i\partial^\mu \gamma_\mu + \mu_5 \bar{\psi} \gamma_0 \gamma_5 \psi) \psi + \mathcal{L}_4, \quad (1)$$

with ψ being a quark field with Dirac, color and flavor indices. In this equation μ_5 is the chiral chemical potential, and its conjugated quantity is the chiral charge density, $n_5 \equiv n_R - n_L$: a finite μ_5 induces a chiral density in the system, and in general the relation between n_5 and μ_5 has to be computed numerically within some model, see for example [25, 26].

In Eq.(1) \mathcal{L}_4 corresponds to the interaction term, namely

$$\mathcal{L}_4 = G \int d^4y d^4z F^*(y-x) F(z-x) \bar{\psi}(y) \psi(z). \quad (2)$$

The interaction term in Eq. (2) is formally equivalent to a local NJL interaction,

$$\mathcal{L}_4 = G(\bar{\Psi}(x)\Psi(x))^2, \quad (3)$$

written in terms of the dressed quark fields

$$\Psi(x) \equiv \int d^4y F(y-x) \psi(y). \quad (4)$$

Chiral symmetry is spontaneously broken by the interaction in Eq. (2); this leads to a nonvanishing expectation value of the dressed quark field operator

$$\sigma \equiv G \langle \bar{\Psi}(x)\Psi(x) \rangle \neq 0. \quad (5)$$

Working at finite temperature T within the well established imaginary time formalism, the thermodynamic potential per unit volume can be written as

$$\Omega = \frac{\sigma^2}{G} - N_c N_f T \sum_n \int \frac{d^3\mathbf{p}}{(2\pi)^3} \log \beta^4 (\omega_n^2 + E_+^2) (\omega_n^2 + E_-^2), \quad (6)$$

where $\beta = 1/T$ and we have defined

$$E_\pm^2 = (p \pm \mu_5)^2 + M(\omega_n, \mathbf{p})^2. \quad (7)$$

Here $\omega_n = \pi T(2n+1)$ corresponds to the fermionic Matsubara frequency and $M(\omega_n, \mathbf{p})$ denotes the quark mass function to be specified later.

2.2. Quark mass functions

In Eq. (7) we have introduced the quark mass function

$$M(p) \equiv -2\sigma\mathcal{C}(p), \quad (8)$$

with $\mathcal{C}(p) \equiv F^2(p)$ and $F(p)$ corresponding to the Fourier transform of the form factor F in Eq. (4). The above equation agrees with the results from one-gluon exchange inspired models [56, 57, 51, 52, 59, 58]. Nonlocal models mimic the constituent quark mass function of QCD in presence of spontaneous chiral symmetry breaking [54, 59] for large p_E . In this work we assume several specific functional forms for $M(p)$ in Eq. (8).

A class of form factors that we use have the form

$$\mathcal{C}(p_E^2) = \theta(\Lambda^2 - p_E^2) + \theta(p_E^2 - \Lambda^2) \frac{\Lambda^2 (\log \Lambda^2 / \Lambda_{QCD}^2)^\gamma}{p_E^2 (\log p_E^2 / \Lambda_{QCD}^2)^\gamma}. \quad (9)$$

For the exponent γ in Eq.(9) we consider here three cases: $\gamma = 0$ for its simplicity; $\gamma = 1$ following [56, 57]; finally $\gamma = 1 - d_m$, inspired by the quark mass function derived by Politzer [54], where $d_m = 12/29$ corresponds to the anomalous mass dimension for $N_f = 2$.

We also consider form factors that connect smoothly the infrared and the ultraviolet p_E domains. In particular, we consider a Yukawa-type form factor, namely [51, 52]

$$\mathcal{C}(p_E^2) = \frac{\Lambda^2}{p_E^2 + \Lambda^2}; \quad (10)$$

then we consider a form factor inspired by the Instanton Liquid Model (ILM) of the QCD vacuum, namely [53]

$$\mathcal{C}(p_E^2) = \frac{d^2 p_E^2}{4} \left\{ \frac{d}{dx} [I_0(x)K_0(x) - I_1(x)K_1(x)] \right\}^2, \quad (11)$$

where d corresponds to the typical instanton size $d \approx 0.36$ fm and $x = |p_E|d/2$. Finally we consider a nonlocal kernel used in nonlocal NJL model studies [56, 57], namely

$$\mathcal{C}(p_E^2) = \theta(\Lambda^2 - p_E^2) e^{-p_E^2 d^2/2} + \theta(p_E^2 - \Lambda^2) \frac{\Lambda^2 (\log \Lambda^2 / \Lambda_{QCD}^2)}{p_E^2 (\log p_E^2 / \Lambda_{QCD}^2)} e^{-\Lambda^2 d^2/2}, \quad (12)$$

where d corresponds to the instanton size used in Eq. (11) and $\Lambda = O(1)$ GeV. Equation (12) offers a smooth version of the form factor in Eq. (9) with $\gamma = 1$.

3. The critical temperature and the order of the phase transition

In this Section we compute the critical line for chiral symmetry restoration as a function of the chiral chemical potential, both within a GL expansion of the thermodynamic potential in Eq.(6) and within numerical calculations using the full potential.

3.1. Ginzburg-Landau expansion

Close to a second order phase transition we can write Eq.(6) as

$$\Omega - \Omega_0 = \frac{\alpha_2}{2} \sigma^2 + \frac{\alpha_4}{4} \sigma^4 + O(\sigma^6), \quad (13)$$

where we have subtracted the thermodynamic potential at $\sigma = 0$, namely Ω_0 ; α_2 and α_4 can be computed by taking the derivatives of Ω with respect to σ at $\sigma = 0$. We find

$$\begin{aligned} \alpha_2 &= \frac{2}{G} - N_c N_f T \sum_n \int \frac{d^3 \mathbf{p}}{(2\pi)^3} \mathcal{C}^2(\omega_n, \mathbf{p}) \\ &\quad \times \frac{16(\mathbf{p}^2 + \omega_n^2 + \mu_5^2)}{[\omega_n^2 + (p - \mu_5)^2][\omega_n^2 + (p + \mu_5)^2]}, \end{aligned} \quad (14)$$

and

$$\alpha_4 = -N_c N_f T \sum_n \int \frac{d^3 \mathbf{p}}{(2\pi)^3} \mathcal{C}^4(\omega_n, \mathbf{p}) \frac{-384[\mathbf{p}^4 + 2\mathbf{p}^2(\omega_n^2 + 3\mu_5^2) + (\mu_5^2 + \omega_n^2)^2]}{[\omega_n^2 + (p - \mu_5)^2]^2 [\omega_n^2 + (p + \mu_5)^2]^2}. \quad (15)$$

The nontrivial solution of the gap equation, $\partial\Omega/\partial\sigma = 0$, for $T \leq T_c$ is given by

$$\sigma^2(T, \mu_5) = -\frac{\alpha_2(T, \mu_5)}{\alpha_4(T, \mu_5)}, \quad (16)$$

and the critical temperature is defined by the condition $\alpha_2(T, \mu_5) = 0$.

In Fig. 1a we plot the coefficient α_2 in units of the parameter Λ^2 as a function of temperature, for three different values of μ_5 . For each value of μ_5 the critical temperature T_c corresponds to $\alpha_2(T_c) = 0$. We show data for the nonlocal model with mass function given by Eqs. (9) and (8) with $\gamma = 0$ and $\Lambda = 900$ MeV; for other models we obtain qualitatively the same results. We notice that increasing μ_5 results in an increasing critical temperature. We also notice that the slope of α_2 at $T = T_c$ increases with μ_5 . Together with the behaviour of α_4 discussed below, this is a signature of the phase transition becoming sharper with μ_5 .

In Fig. 1b we plot the coefficient α_4 versus temperature, for the same values of μ_5 shown in Fig. 1a of the figure. We notice that for any value of μ_5 the coefficient α_4 decreases in magnitude, but it is always positive at the critical temperature meaning the phase transition is a second order one. We also notice that the magnitude of α_4 at $T = T_c(\mu_5)$ decreases compared to the case $\mu_5 = 0$, implying that the phase transition becomes sharper with increasing μ_5 . In fact because of Eq. (16) we can write the solution of the gap equation for $T \approx T_c$ as

$$\sigma^2 = -\frac{1}{\alpha_4(T_c)} \left. \frac{d\alpha_2}{dT} \right|_{T=T_c} (T - T_c) + O[(T - T_c)^2], \quad (17)$$

then the slope of the condensate at the critical temperature is given by

$$\left. \frac{d\sigma^2}{dT} \right|_{T=T_c} = -\frac{1}{\alpha_4(T_c)} \left. \frac{d\alpha_2}{dT} \right|_{T=T_c}, \quad (18)$$

which becomes larger as we increase μ_5 because α_4 decreases and the slope of α_2 at the critical temperature increases with μ_5 . Our conclusion is that within the range of μ_5 explored in our study, we have a firm signal that the phase transition becomes sharper as μ_5 is increased, but there is no critical endpoint because α_4 does not change sign at the critical temperature. This is in agreement with lattice simulations [30, 31] but it is in disagreement with previous model studies which used a different regularization scheme [24, 26, 25, 27], showing how the existence of the critical point in the phase diagram is very sensitive on the regularization prescription, in fact already noticed in [28]. Finally in Fig. 1c we plot the coefficient α_4 at $T = T_c(\mu_5)$ for several models. We notice that although the numerical value of α_4 strongly depends on the model, we find that it is always positive at $T = T_c$.

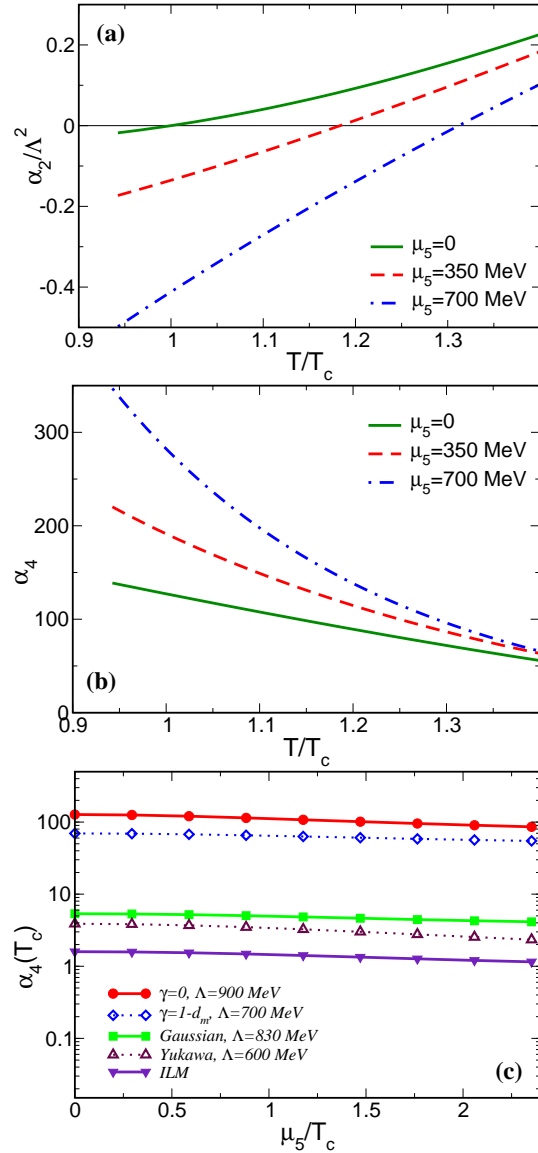


Figure 1. (a). Coefficient α_2 in units of the parameter Λ^2 as a function of temperature, for three different values of μ_5 . For each value of μ_5 the critical temperature T_c corresponds to $\alpha_2(T_c) = 0$. (b). Coefficient α_4 versus temperature, for three different values of μ_5 . (a) and (b) refer to the nonlocal model with mass function given by Eqs. (9) and (8) with $\gamma = 0$ and $\Lambda = 900$ MeV. (c). Evolution of the coefficient α_4 computed at $T = T_c(\mu_5)$ versus μ_5 for several models.

3.2. Beyond Ginzburg-Landau expansion

In the previous subsection we have discussed results obtained within a GL expansion of the thermodynamic potential, see Eq. (13). The GL expansion is a useful tool because it allows to study the analytical behaviour of the thermodynamic potential close to the phase transition. As long as we are interested to the critical temperature at a second order phase transition the GL expansion is equivalent to use the full thermodynamic potential in Eq. (6): as a matter of fact, it requires a straightforward calculation to

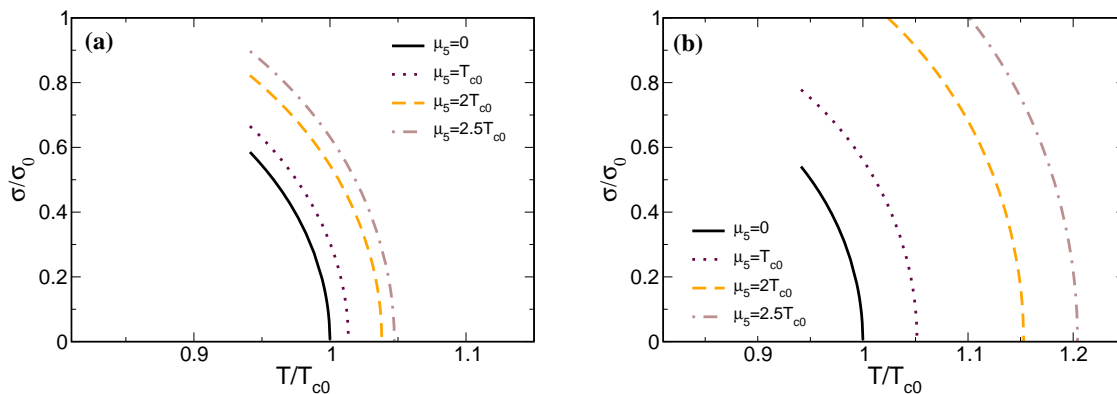


Figure 2. (a). NJL condensate, defined in Eq. (5), versus temperature for several values of μ_5 , for the case of the Gaussian form factor of Fig. 3. (b). Condensate for the case of the Yukawa form factor with $\Lambda = 900$ MeV in Fig. 3. In both panels T_{c0} corresponds to the critical temperature at $\mu_5 = 0$, while σ_0 denotes the condensate at $T = 0$ and $\mu_5 = 0$. For both form factors we plot data for several values of μ_5 : in particular black solid lines correspond to $\mu_5 = 0$, maroon dotted lines to $\mu_5 = T_{c0}$, orange dashed lines to $\mu_5 = 2T_{c0}$, finally brown dot-dashed lines to $\mu_5 = 2.5T_{c0}$.

verify that the gap equation $\partial\Omega/\partial\sigma = 0$ at $T = T_c$ obtained from Eq. (13) coincides with the GL gap equation at $T = T_c$, that is $\alpha_2 = 0$ where α_2 is the second order GL coefficient in Eq. (13). On the other hand, for a first order phase transition the GL expansion is not reliable because the value of the condensate at $T = T_c$ might not be small compared to T , and the use of the expansion in Eq. (13) might be doubtful.

A natural question therefore arises, namely if the above results, in particular the order of the phase transition, are a mere consequence of the GL expansion or if they are in agreement with those that would be obtained using the gap equation derived from the full thermodynamic potential. In the previous Section we have first computed the temperature at which $\alpha_2 = 0$, identifying this with T_c , then we have computed α_4 at $T = T_c$ checking its sign: we have then concluded that being $\alpha_4 > 0$ the phase transition is always of the second order regardless the value of μ_5 ; within the GL approximation $\alpha_4 < 0$ would have been a signal of a first order phase transition. The purpose of this Section is to check the results of the previous Section going beyond the GL expansion of Eq. (13). To this end we compute the condensate defined in Eq. (5) by solving the gap equation $\partial\Omega/\partial\sigma = 0$ with Ω defined in Eq. (6).

In Fig. 2 we plot the condensate versus temperature for two of the nonlocal NJL models mentioned in Fig. 3, namely the Gaussian model (a) and the Yukawa model with $\Lambda = 900$ MeV (b). We have checked that for the other models we obtain similar results. In the figure T_{c0} corresponds to the critical temperature at $\mu_5 = 0$, while σ_0 denotes the condensate at $T = 0$ and $\mu_5 = 0$. For both form factors we plot data for several values of μ_5 : in particular black solid lines correspond to $\mu_5 = 0$, maroon dotted lines to $\mu_5 = T_{c0}$, orange dashed lines to $\mu_5 = 2T_{c0}$, finally brown dot-dashed lines to $\mu_5 = 2.5T_{c0}$. For both cases we have zoomed to the temperature range close to the critical temperature

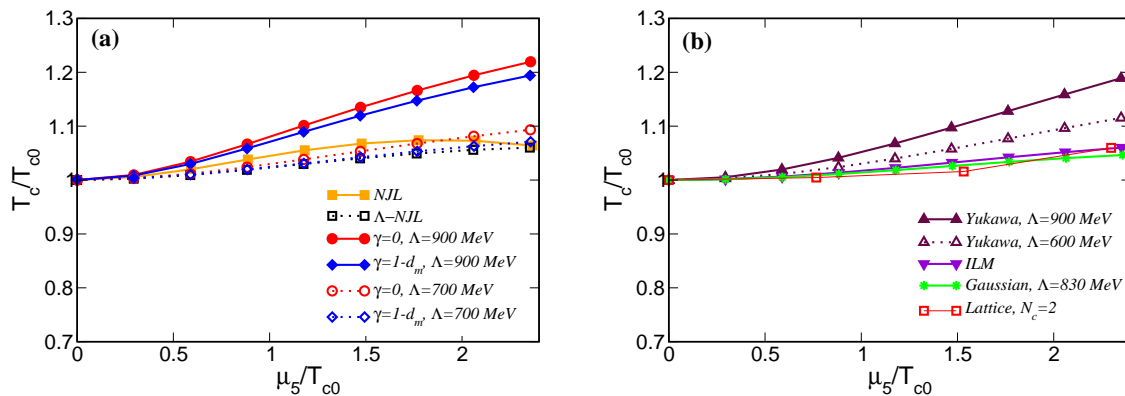


Figure 3. (a). Critical temperature for chiral symmetry restoration versus μ_5 for several running mass models described in the text. Squares correspond to NJL and Λ -NJL models with a 4D sharp cutoff $\Lambda = 900$ MeV. Circles correspond to mass function given by Eqs. (9) and (8) with $\gamma = 0$, for two different values of Λ ; diamonds correspond to the same mass function with $\gamma = 1 - d_m$. (b). Critical temperature for chiral symmetry restoration versus μ_5 for several running mass models described in the text. Data with triangles pointing upwards correspond to a Yukawa-like form factor in Eq. (10) with two values of Λ . Data denoted by triangles pointing downwards correspond to the Instanton Liquid Model (ILM) form factor in Eq. (11). Stars correspond to the nonlocal form factor in Eq. (12). Lattice data for $N_c = 2$ have been adapted from [31]. In both panels T_{c0} corresponds to critical temperature at $\mu_5 = 0$.

which is the one relevant for our study.

Data shown in Fig. 2 confirm the results obtained within the GL expansion and presented in the previous subsection. In fact, the critical temperature is found to increase with μ_5 . Moreover the condensate vanishes smoothly with increasing temperature, meaning the phase transition is of the second order (a first order phase transition would appear as a discontinuity in the condensate, which we do not find for all the values of μ_5 explored here). We thus can conclude that the main results of the our study, with particular regard to the absence of a first order phase transition line in the $\mu_5 - T$ plane, are not a mere consequence of the GL expansion Eq. (13). The presence of a first order phase transition line, found in NJL and quark-meson model calculations [24, 25, 26, 27] but not found in the nonlocal NJL model calculations, appears thus to be model dependent, in agreement with what anticipated in [28].

3.3. The critical line in the $\mu_5 - T$ plane

In Fig. 3 we plot the critical temperature versus μ_5 for the nonlocal models described in the text. In the figure T_{c0} denotes the critical temperature at $\mu_5 = 0$. In Fig. 3a we collect the results for the sharp models described in the text. Circles correspond to mass function given by Eqs. (9) and (8) with $\gamma = 0$, for two different values of Λ ; diamonds correspond to the same mass function with $\gamma = 1 - d_m$. In Fig. 3a we have also shown the results for two local NJL models. In particular, we denote by squares the

results for a standard local NJL model with a 4-dimensional sharp cutoff on the vacuum term and no cutoff on the thermal part of the free energy; moreover, empty squares correspond to a model dubbed Λ -NJL, in which there is a 4D sharp cutoff both on the vacuum and on the thermal contribution to the gap equation. In both cases $\Lambda = 900$ MeV. In Fig. 3b we plot the critical temperature for smooth form factors. In particular data with triangles pointing upwards correspond to a Yukawa-like form factor in Eq. (10) with two values of Λ . Data denoted by triangles pointing downwards correspond to the Instanton Liquid Model (ILM) form factor in Eq. (11). Finally stars correspond to the nonlocal form factor in Eq. (12). In both panels both temperature and chemical potential are measured in units of the critical temperature at $\mu_5 = 0$. In each calculation we have fixed the value of the parameter Λ in the form factor, then we have tuned the NJL coupling constant G in order to obtain $T_{c0} = 170$ MeV for any model.

The results in Fig. 3 show that for all the nonlocal models studied in this article the critical temperature increases with μ_5 . For large values of μ_5 the results shown in Fig. 3 should be not considered very reliable because we have neglected a possible backreaction on the nonlocal interaction kernel due to μ_5 . For the case of local models, we find that the Λ -NJL model still predicts T_c increases with μ_5 , at least up to values of μ_5 of the order of Λ . This is in agreement with the previous analysis of [28] where a Λ -NJL with a 3-dimensional cutoff has been considered. For the NJL model result in Fig. 3 we find that T_c increases with μ_5 for small values of μ_5 , in agreement with a small μ_5 analysis presented in the following section.

A detailed comparison with lattice data [30, 31] is premature because those data have not been obtained in the chiral limit; moreover, some data on the lattice correspond to $N_c = 2$ QCD while here we consider $N_c = 3$. However, we can at least compare the magnitude of the increase of the critical temperature obtained within the nonlocal models and within the lattice simulations. In Fig. 3 we show lattice results for $T_c(\mu_5)$ for $N_c = 2$ adapted from Ref. [31] in which the critical temperature at $\mu_5 = 0$ is $T_{c0} = 195.8 \pm 0.4$ MeV. We find that among the models considered here, the ones with Gaussian ILM form factors, respectively Eqs. (12) and (11), better reproduce the magnitude of the variation of the critical temperature with μ_5 .

4. Small μ_5 analysis

Since the phase transition is of the second order we can use the GL expansion, see Eq. (13), to investigate in more detail the relation between μ_5 and T_c within the model at hand. In particular, we perform in this section a small μ_5 analysis of the coefficient α_2 in Eq. (13) to enlighten the differences between local and nonlocal NJL models at finite μ_5 .

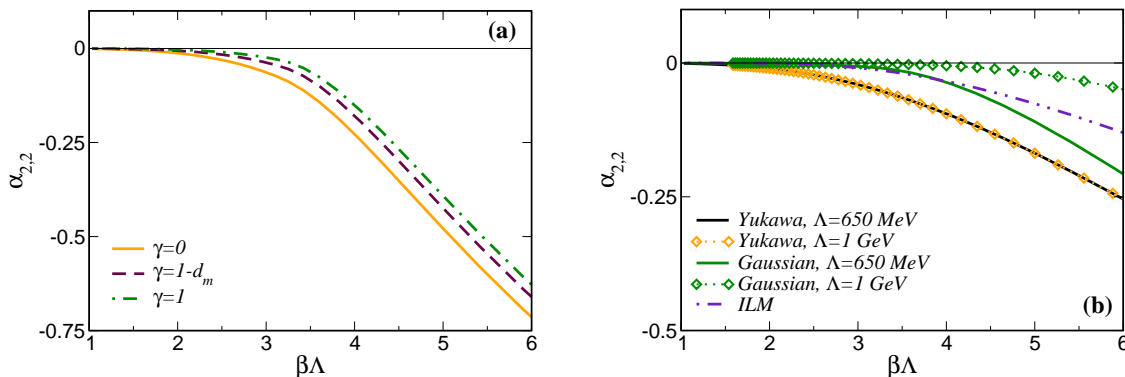


Figure 4. (a). Coefficient $\alpha_{2,2}$ versus $\beta\Lambda$ obtained within the nonlocal 4D model with the quark mass function specified by Eqs.(9) and(8). (b). Coefficient $\alpha_{2,2}$ versus $\beta\Lambda$ obtained within the nonlocal 4D model with the quark mass function specified by Yukawa-like form factor Eq.(10), nonlocal NJL form factor in Eq.(12) and Instanton Liquid Model form factor in Eq.(11). For the latter we have introduced a fictitious scale $\Lambda = 650$ MeV on abscissas in order to make comparison with other models easier.

4.1. The coefficient $\alpha_{2,2}$ and T_c versus μ_5 for $\mu_5/T \ll 1$

We expand

$$\alpha_2 = \alpha_{2,0} + \mu_5^2 \alpha_{2,2}. \quad (19)$$

The above equation allows to compute, to the lowest order in μ_5/T , the shift of the critical temperature due to μ_5 :

$$\delta T_c = -\frac{\alpha_{2,2}(T_c^0)}{a} \mu_5^2, \quad (20)$$

where T_c^0 corresponds to the critical temperature at $\mu_5 = 0$ and $a \equiv d\alpha_{2,0}/dT$ at $T = T_c^0$. The quantity a depends on the specific model used but it is positive by definition because $\alpha_{2,0}$ is negative for $T < T_c$ and positive for $T > T_c$, thus the sign of δT in Eq. 20 is determined only by the sign of $\alpha_{2,2}$. A straightforward computation starting from Eq.(6) shows that

$$\alpha_{2,2} = -4N_c N_f T \sum_n \int \frac{d^3 \mathbf{p}}{(2\pi)^3} \mathcal{C}^2(\omega_n, \mathbf{p}) \frac{2(3\mathbf{p}^2 - \omega_n^2)}{(\mathbf{p}^2 + \omega_n^2)^3}, \quad (21)$$

where \mathcal{C} is the non local interaction kernel. Once $\alpha_{2,2}$ is known, the critical temperature versus μ_5 can be computed as

$$T_c(\mu_5) = T_c^0 \left[1 - \frac{\alpha_{2,2}(T_c^0)}{a T_c^0} \mu_5^2 \right]. \quad (22)$$

In Figure 4 we plot the coefficient $\alpha_{2,2}$ computed by Eq.(21) for the several form factors described in Section 2. For all the models of p_E -dependent quark mass functions we find that $\alpha_{2,2} < 0$, and because of Eq.(22) this implies μ_5 tends to increase the critical temperature for chiral symmetry restoration within the model at hand. This is different from what is obtained within local models in which critical temperature has been found to decrease with μ_5 , with the exception of [23] where renormalization has been used to treat the divergent vacuum term.

4.2. The modes contributions

It is instructive to present an analysis of the coefficient $\alpha_{2,2}$ defined in Eq. (21), in order to enlighten the difference between the nonlocal and local models for what concerns $T_c(\mu_5)$ for small values of μ_5 . This analysis follows a similar one presented in [28] for the case of an NJL model with a local interaction kernel and a 3-dimensional cutoff. For simplicity, we focus on the form factor given by Eq.(9) with $\gamma = 0$ which allows easier manipulations and a clearer mode separation. We split $\alpha_{2,2}$ as

$$\alpha_{2,2} = \mathcal{I}_1 + \mathcal{I}_2 + \mathcal{J}_1 + \mathcal{J}_2; \quad (23)$$

here we have introduced several contributions depending on the momentum region of quarks and on temperature. These terms are defined as follows. Firstly we add and subtract the $T = 0$ contribution to Eq. (21), that according to the well known rules of finite temperature field theory in the imaginary time formalism reads

$$\alpha_{2,2}^0 = -4N_c N_f \int \frac{d^4 \mathbf{p}_E}{(2\pi)^4} \mathcal{C}^2(p_E) \frac{2(3\mathbf{p}^2 - p_4^2)}{(\mathbf{p}^2 + p_4^2)^3}; \quad (24)$$

then we define

$$\mathcal{I}_1 = -4N_c N_f \int_{p_E^2 \leq \Lambda^2} \frac{d^4 \mathbf{p}_E}{(2\pi)^4} \mathcal{C}^2(p_E) \frac{2(3\mathbf{p}^2 - p_4^2)}{(\mathbf{p}^2 + p_4^2)^3}, \quad (25)$$

$$\mathcal{I}_2 = -4N_c N_f \int_{p_E^2 > \Lambda^2} \frac{d^4 \mathbf{p}_E}{(2\pi)^4} \mathcal{C}^2(p_E) \frac{2(3\mathbf{p}^2 - p_4^2)}{(\mathbf{p}^2 + p_4^2)^3}, \quad (26)$$

which correspond to the contributions to $\alpha_{2,2}$ at zero temperature of the modes with $p_E^2 \leq \Lambda^2$ and $p_E^2 > \Lambda^2$ respectively. Moreover we define

$$\begin{aligned} \mathcal{J}_1 = & -4N_c N_f T \sum_n \int \frac{d^3 \mathbf{p}}{(2\pi)^3} \mathcal{C}^2(\omega_n, \mathbf{p}) \frac{2(3\mathbf{p}^2 - \omega_n^2)}{(\mathbf{p}^2 + \omega_n^2)^3} \Big|_{\omega_n^2 + \mathbf{p}^2 \leq \Lambda^2} \\ & + 4N_c N_f \int_{p_E^2 \leq \Lambda^2} \frac{d^4 \mathbf{p}_E}{(2\pi)^4} \mathcal{C}^2(p_E) \frac{2(3\mathbf{p}^2 - p_4^2)}{(\mathbf{p}^2 + p_4^2)^3}, \end{aligned} \quad (27)$$

$$\begin{aligned} \mathcal{J}_2 = & -4N_c N_f T \sum_n \int \frac{d^3 \mathbf{p}}{(2\pi)^3} \mathcal{C}^2(\omega_n, \mathbf{p}) \frac{2(3\mathbf{p}^2 - \omega_n^2)}{(\mathbf{p}^2 + \omega_n^2)^3} \Big|_{\omega_n^2 + \mathbf{p}^2 > \Lambda^2} \\ & + 4N_c N_f \int_{p_E^2 > \Lambda^2} \frac{d^4 \mathbf{p}_E}{(2\pi)^4} \mathcal{C}^2(p_E) \frac{2(3\mathbf{p}^2 - p_4^2)}{(\mathbf{p}^2 + p_4^2)^3}, \end{aligned} \quad (28)$$

which correspond to the contributions to $\alpha_{2,2}$ at finite temperature of the modes with $p_E^2 \leq \Lambda^2$ and $p_E^2 > \Lambda^2$ respectively.

Evaluation of integrals and summation over Matsubara frequencies in the above equations lead to the following results:

- modes with $p_E^2 \leq \Lambda^2$ at $T = 0$:

$$\mathcal{I}_1 = -a_2 \frac{4N_c N_f}{2\pi^2} \log \frac{\Lambda}{m_0}; \quad (29)$$

- modes with $p_E^2 > \Lambda^2$ at $T = 0$:

$$\mathcal{I}_2 = -a_1 \frac{4N_c N_f}{2\pi^2}; \quad (30)$$

- modes with $p_E^2 \leq \Lambda^2$ at $T > 0$:

$$\mathcal{J}_1 = \frac{4N_c N_f}{2\pi^2} \left[a_2 \log \frac{1}{\beta m_0} + |F(\beta\Lambda)| \right]; \quad (31)$$

- modes with $p_E^2 > \Lambda^2$ at $T > 0$:

$$\mathcal{J}_2 = \frac{4N_c N_f}{2\pi^2} |G(\beta\Lambda)|; \quad (32)$$

in order to obtain the above equations we have done some manipulation on the definitions in Eqs. (26) and (26) which allow to extract the analytical contribution shown in Eqs. (29) - (32). The coefficients $a_1 \approx 0.25$ and $a_2 \approx 0.938$ are the results of numerical integration. Moreover we have introduced an infrared cutoff m_0 which appears in the intermediate steps of the computation when the contributions are split; this fictitious cutoff disappears when the sum of the contributions is done, as it is clear from Eqs.(31) and (29). In Fig. 5a we plot the functions F , G as well as their sum in order to understand the role of the several terms in Eq.(23). In particular the modes in Eq.(30) come from the high momentum part of the Dirac sea; they are not usually considered in a local model calculation because in that case their contribution is divergent hence it is simply subtracted. We notice that this contribution to $\alpha_{2,2}$ is negative, thus it helps to keep the critical temperature at finite μ_5 higher than that at $\mu_5 = 0$.

4.3. Comparison with local NJL model

The benefit of expansion in Eq. (23) is that it allows to compare easily nonlocal with local models. To this end we introduce a local Λ -NJL model in which we remove all the modes with $p_E^2 > \Lambda^2$; the coefficient $\alpha_{2,2}$ will be thus given by the sum of Eqs. (29) and (31) namely

$$\alpha_{2,2}^{\Lambda\text{-NJL}} = -\frac{4N_c N_f}{2\pi^2} [a_2 \log \beta\Lambda - |F(\beta\Lambda)|]. \quad (33)$$

We also introduce the standard local NJL model in which we remove the ultraviolet modes $p_E^2 > \Lambda^2$ only at $T = 0$, and integrate over all momenta at finite temperature:

$$\alpha_{2,2}^{\text{NJL}} = -\frac{4N_c N_f}{2\pi^2} [a_2 \log \beta\Lambda - |F(\infty)|], \quad (34)$$

where $F(\infty) \equiv \lim_{x \rightarrow \infty} F(x)$. Both these models follow the definitions already introduced in [28].

In Fig. 5b we plot the coefficient $\alpha_{2,2}$ for the the local NJL model (gren dot-dashed line), the local Λ -NJL model (maroon dashed line) and the nonlocal model with mass function given by Eqs. (9) and (8) with $\gamma = 0$. For the local models there exists a window of $\beta\Lambda$ in which $\alpha_{2,2} > 0$; on the other hand for the nonlocal model considered here we find $\alpha_{2,2} < 0$ for any value of $\beta\Lambda$. The fact that $\alpha_{2,2}$ can be positive in the local models is in part due to the absence of the vacuum term in Eq. (30) which would give a negative contribution to $\alpha_{2,2}$. Moreover, the main difference between the standard local NJL and the Λ -NJL models is that in the latter the positive contribution \mathcal{J}_2 of the modes with $p_E^2 > \Lambda^2$ at finite temperature is missing, while in the former the positive

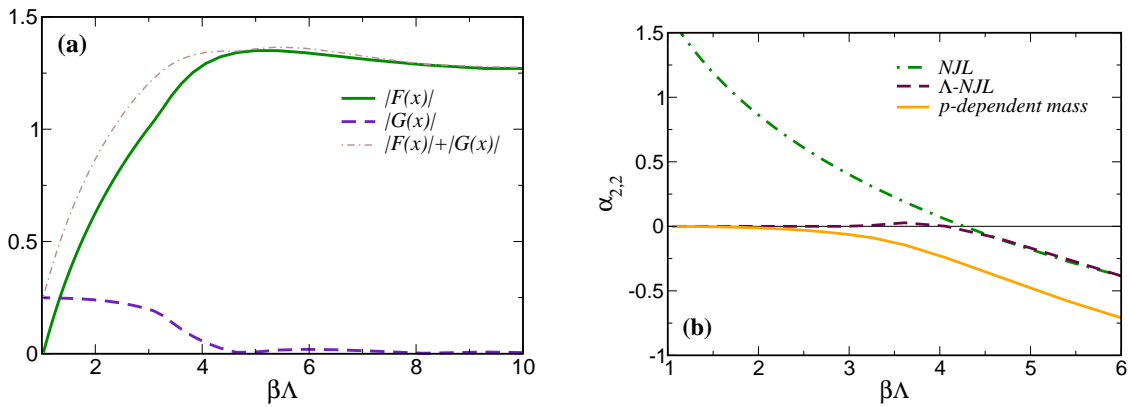


Figure 5. (a). Functions $F(x)$, $G(x)$ and their sum. (b). Comparison of the $\alpha_{2,2}$ coefficients for the standard local NJL model (green dot-dashed line), the Λ -NJL model (maroon dashed line) and the nonlocal model with mass function given by Eqs.(9) and(8) with $\gamma = 0$.

contribution of these modes is added assuming a constant mass function: this explains why $\alpha_{2,2}$ for the Λ -NJL model is always smaller than the one of the standard local NJL.

The difference between the nonlocal model on the one hand, and the local models on the other hand, is that for the former we find $\alpha_{2,2}$ is always negative, while for the latter there exist windows of $\beta\Lambda$ in which $\alpha_{2,2}$ is positive. This means that depending on the values of T_c and Λ , T_c can either increase or decrease with μ_5 in local NJL models, the result depending on model parameters. The parameter window in which $\alpha_{2,2}$ is positive (implying T_c decreasing with μ_5) is very tiny for the Λ -NJL model, but it is quite wide for the standard local NJL model. Considering that for the 4-dimensional regularization typically $\Lambda \approx 1$ GeV and T_c is in the range 150 – 200 MeV, the value of $\beta\Lambda$ at $T = T_c$ turns out to be approximately in the range 5 – 6.7: in this range we find that $\alpha_{2,2}$ is negative, which explains why in this work we find that T_c increases with μ_5 also in the case of the local models.

In Fig. 6 we plot $\alpha_{2,2}$ computed for a 3-dimensional regulator; the calculation steps are similar to those of the models with 4-dimensional regulator so we do not repeat them. In particular the green dot-dashed line corresponds to the model used in [24, 25, 27]. For 3-dimensional regularizations the value of Λ is considerably smaller than the one used in the 4-dimensional case, typically of the order of 600 MeV [43, 44, 45] while the range in which T_c runs is the same found in the 4-dimensional case. This implies that $\beta\Lambda$ at $T = T_c$ for 3-dimensional regularization schemes are in the range 3 – 4: for the case of the local NJL model we find this range to be in the region where $\alpha_{2,2}$ is positive, see green dot-dashed line in Fig 6, meaning that T_c is lowered by μ_5 . Similarly for the case of the Λ -NJL model we find that $\alpha_{2,2}$ is negative implying that T_c increases with μ_5 . Comparing the results for the standard local NJL models with 4-dimensional and 3-dimensional regulators we thus conclude that in previous calculations [24, 25, 27] the critical temperature decreases with μ_5 because of an accident driven by the model

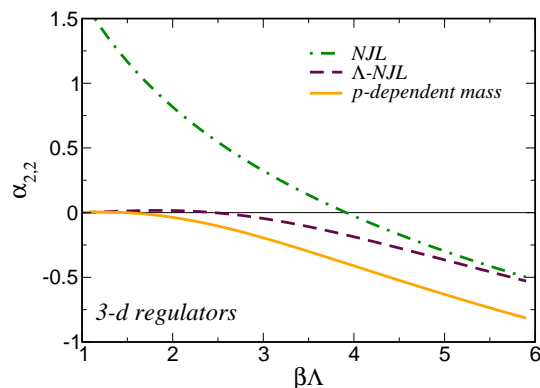


Figure 6. Comparison of $\alpha_{2,2}$ for the standard local NJL model (green dot-dashed line), the Λ -NJL model (maroon dashed line) and the nonlocal model with mass function given by Eqs.(9) and(8) with $\gamma = 0$. In all models we have used either a 3-dimensional regulator or a quark mass function depending on 3-momentum.

parameters, suggesting that behaviour of T_c to be an artifact of the 3-dimensional regularization.

5. Conclusions

In this article we have presented a model study of the critical temperature of chiral symmetry restoration, T_c , as a function of chiral chemical potential, μ_5 . We have used a nonlocal NJL model with several Euclidean interaction kernels, chosen to mimick the constituent quark mass of QCD in the ultraviolet.

We have studied the thermodynamic potential both within a Ginzburg-Landau expansion in the vicinity of the second order critical line, and within calculations using the full potential. The main interest of our study has been the computation of the critical temperature versus μ_5 . The results about $T_c(\mu_5)$ are collected in Fig. 3 for the different models. We have found that within the nonlocal models used in our study, T_c increases with μ_5 regardless of the interaction kernel used. We remark that our interaction kernels lack of a backreaction of μ_5 , hence our results should be taken with a grain of salt for $\mu_5 = O(1 \text{ GeV})$, while they are reliable for smaller values of μ_5 . We have also found that T_c increases with μ_5 for a standard NJL model with a 4-dimensional regulator, at least for small values of μ_5 . According to these findings, we have concluded that previous works [24, 25, 26, 27] found T_c a decreasing function of μ_5 as a result of an accident driven by the model parameters, suggesting that behaviour of T_c to be an artifact of the 3-dimensional regularization of the standard local NJL model.

We have then checked the order of the phase transition by computing the coefficient α_4 of the GL effective potential: we have found that although μ_5 makes the transition sharper because the magnitude of α_4 decreases with μ_5 at T_c , the coefficient never vanishes as it should happen at the critical endpoint. We have confirmed the results obtained within the GL expansion by performing a calculation considering the full

thermodynamic potential. Our conclusion is that there is no trace of a critical endpoint in the phase diagram, at least within the range of μ_5 we have explored in this article. According to this result we can conclude that the presence of the critical point in the $\mu_5 - T$ plane advertised before [24, 25, 26, 27] is model dependent: in particular its existence depends on the details of the interaction used in the model calculation. This result, as well as our conclusion about $T_c(\mu_5)$, agree with [28].

We would like to close this article by doing few considerations about the implications of our study. The main purpose of our investigation is purely theoretical: the interest of a phase diagram of QCD in the $\mu_5 - T$ plane was suggested in several references [24, 25, 26, 27], where it was found that the critical temperature for chiral symmetry restoration and for confinement-deconfinement decrease with μ_5 , and a critical endpoint appears in the phase diagram. Since both these characteristics belong also to the would-be phase diagram of QCD in the $\mu - T$ plane, and because the $\mu_5 - T$ plane can be accessed by Lattice QCD calculations while QCD at finite μ suffers the sign problem, the idea that might derive from [24, 25, 26, 27] is that Lattice QCD studies at finite μ_5 can shed a light on QCD in the $\mu - T$ plane. Therefore the main purpose of our model study has been to check whether the predictions of [24, 25, 26, 27] are general or specific to the model used in the calculations. What we have found is that the latter scenario is actually verified, since classes of effective models exist in which the phase diagram looks quite different from that advertised previously. The scenario depicted here is in agreement with Lattice QCD calculations [30, 31], and with results obtained by solving Schwinger-Dyson equations at finite μ_5 [34, 35]. Therefore we can conclude by stating that we have now three independent calculation schemes that agree on the fact that T_c increases with μ_5 , and that the transition line is of the second order. As a consequence it seems unlikely that further investigations at finite μ_5 can teach something about the QCD phase structure in the $\mu - T$ plane.

Regarding the confinement-deconfinement in the $\mu_5 - T$ plane, Lattice QCD has found no evidence for a split of this crossover from the chiral crossover [30, 31]. In order to study this problem within the models at hand we should augment the NJL model with some physical quantity that is sensitive to the deconfinement: the best candidate model is the NJL model augmented with a coupling to the Polyakov loop (PNJL) [60, 61]. We expect that the picture drawn in this article does not change drastically by turning to the PNJL model, in particular if a coupling between the NJL interaction and the Polyakov loop is taken into account [62, 63]. A study of the problems studied in our article by means of the PNJL model might be the subject of a future study. Moreover, the absence of a critical endpoint in the $\mu_5 - T$ plane might limit the inhomogeneous condensates that have been predicted to develop in the $\mu - T$ plane near the critical point, see for example [64, 65, 66, 67]. More study related to this topic might be worth of an investigation.

Finally, we would like to mention that during the very final stage of preparation of the present manuscript, Ref. [68] appeared in which the same problem has been studied and an increasing T_c versus μ_5 has been found, in agreement with the results presented

in this article. Moreover during the revision of the manuscript Ref. [69] appeared, in which similar conclusions to the work presented here as well as to that of [28] have been drawn, regarding $T_c(\mu_5)$ and the order of the phase transition at finite μ_5 .

Acknowledgments. The authors would like to thank the CAS President's International Fellowship Initiative (Grant No. 2015PM008), and the NSFC projects (11135011 and 11575190). M. R. also acknowledges discussions with M. Frasca.

References

- [1] S. L. Adler, Phys. Rev. **177**, 2426 (1969).
- [2] J. S. Bell and R. Jackiw, Nuovo Cim. A **60**, 47 (1969).
- [3] G. D. Moore, hep-ph/0009161.
- [4] G. D. Moore and M. Tassler, JHEP **1102**, 105 (2011).
- [5] D. E. Kharzeev, L. D. McLerran and H. J. Warringa, Nucl. Phys. A **803**, 227 (2008).
- [6] K. Fukushima, D. E. Kharzeev and H. J. Warringa, Phys. Rev. D **78**, 074033 (2008).
- [7] D. T. Son and P. Surowka, Phys. Rev. Lett. **103**, 191601 (2009).
- [8] N. Banerjee, J. Bhattacharya, S. Bhattacharyya, S. Dutta, R. Loganayagam and P. Surowka, JHEP **1101**, 094 (2011).
- [9] K. Landsteiner, E. Megias and F. Pena-Benitez, Phys. Rev. Lett. **107**, 021601 (2011).
- [10] D. T. Son and A. R. Zhitnitsky, Phys. Rev. D **70**, 074018 (2004).
- [11] M. A. Metlitski and A. R. Zhitnitsky, Phys. Rev. D **72**, 045011 (2005).
- [12] D. E. Kharzeev and H. U. Yee, Phys. Rev. D **83**, 085007 (2011).
- [13] M. N. Chernodub, JHEP **1601**, 100 (2016).
- [14] M. N. Chernodub and M. Zubkov, arXiv:1508.03114 [cond-mat.mes-hall].
- [15] M. N. Chernodub, A. Cortijo, A. G. Grushin, K. Landsteiner and M. A. H. Vozmediano, Phys. Rev. B **89**, no. 8, 081407 (2014).
- [16] V. Braguta, M. N. Chernodub, K. Landsteiner, M. I. Polikarpov and M. V. Ulybyshev, Phys. Rev. D **88**, 071501 (2013).
- [17] Q. Li *et al.*, arXiv:1412.6543 [cond-mat.str-el].
- [18] A. V. Sadofyev and M. V. Isachenkov, Phys. Lett. B **697**, 404 (2011).
- [19] A. V. Sadofyev, V. I. Shevchenko and V. I. Zakharov, Phys. Rev. D **83**, 105025 (2011).
- [20] Z. V. Khaidukov, V. P. Kirilin, A. V. Sadofyev and V. I. Zakharov, arXiv:1307.0138 [hep-th].
- [21] V. P. Kirilin, A. V. Sadofyev and V. I. Zakharov, arXiv:1312.0895 [hep-th].
- [22] A. Avdoshkin, V. P. Kirilin, A. V. Sadofyev and V. I. Zakharov, Phys. Lett. B **755**, 1 (2016).
- [23] M. Ruggieri and G. X. Peng, arXiv:1602.03651 [hep-ph].
- [24] R. Gatto and M. Ruggieri, Phys. Rev. D **85**, 054013 (2012).
- [25] K. Fukushima, M. Ruggieri and R. Gatto, Phys. Rev. D **81**, 114031 (2010).
- [26] M. N. Chernodub and A. S. Nedelin, Phys. Rev. D **83**, 105008 (2011).
- [27] M. Ruggieri, Phys. Rev. D **84**, 014011 (2011).
- [28] L. Yu, H. Liu and M. Huang, arXiv:1511.03073 [hep-ph].
- [29] L. Yu, J. Van Doorselaere and M. Huang, Phys. Rev. D **91**, no. 7, 074011 (2015).
- [30] V. V. Braguta, E.-M. Ilgenfritz, A. Y. Kotov, B. Petersson and S. A. Skinderev, arXiv:1512.05873 [hep-lat].
- [31] V. V. Braguta, V. A. Goy, E.-M. Ilgenfritz, A. Y. Kotov, A. V. Molochkov, M. Muller-Preussker and B. Petersson, JHEP **1506**, 094 (2015).
- [32] V. V. Braguta and A. Y. Kotov, arXiv:1601.04957 [hep-th].
- [33] M. Hanada and N. Yamamoto, PoS LATTICE **2011**, 221 (2011) [arXiv:1111.3391 [hep-lat]].
- [34] S. S. Xu, Z. F. Cui, B. Wang, Y. M. Shi, Y. C. Yang and H. S. Zong, Phys. Rev. D **91**, no. 5, 056003 (2015).
- [35] B. Wang, Y. L. Wang, Z. F. Cui and H. S. Zong, Phys. Rev. D **91**, no. 3, 034017 (2015).

- [36] D. Ebert, T. G. Khunjua, K. G. Klimenko and V. C. Zhukovsky, *Phys. Rev. D* **93**, no. 10, 105022 (2016).
- [37] S. S. Afonin, A. A. Andrianov and D. Espriu, *Phys. Lett. B* **745**, 52 (2015).
- [38] A. A. Andrianov, D. Espriu and X. Planells, *Eur. Phys. J. C* **73**, no. 1, 2294 (2013).
- [39] X. Planells, A. A. Andrianov, V. A. Andrianov and D. Espriu, *PoS QFTHEP* **2013**, 049 (2013) [arXiv:1310.4434 [hep-ph]].
- [40] C. Manuel and J. M. Torres-Rincon, *Phys. Rev. D* **92**, no. 7, 074018 (2015).
- [41] Y. Nambu and G. Jona-Lasinio, *Phys. Rev.* **122**, 345 (1961).
- [42] Y. Nambu and G. Jona-Lasinio, *Phys. Rev.* **124**, 246 (1961).
- [43] S. P. Klevansky, *Rev. Mod. Phys.* **64**, 649 (1992).
- [44] T. Hatsuda and T. Kunihiro, *Phys. Rept.* **247**, 221 (1994).
- [45] M. Buballa, *Phys. Rept.* **407**, 205 (2005).
- [46] S. M. Schmidt, D. Blaschke and Y. L. Kalinovsky, *Phys. Rev. C* **50**, 435 (1994).
- [47] R. D. Bowler and M. C. Birse, *Nucl. Phys. A* **582**, 655 (1995).
- [48] R. S. Plant and M. C. Birse, *Nucl. Phys. A* **628**, 607 (1998).
- [49] D. Blaschke, G. Burau, Y. L. Kalinovsky, P. Maris and P. C. Tandy, *Int. J. Mod. Phys. A* **16**, 2267 (2001).
- [50] D. Gomez Dumm, D. B. Blaschke, A. G. Grunfeld and N. N. Scoccola, *Phys. Rev. D* **73**, 114019 (2006).
- [51] M. Frasca, *Phys. Rev. C* **84**, 055208 (2011).
- [52] M. Frasca, *JHEP* **1311**, 099 (2013).
- [53] T. Schfer and E. V. Shuryak, *Rev. Mod. Phys.* **70**, 323 (1998).
- [54] H. D. Politzer, *Nucl. Phys. B* **117**, 397 (1976).
- [55] J. Gasser and H. Leutwyler, *Phys. Rept.* **87**, 77 (1982).
- [56] T. Hell, S. Roessner, M. Cristoforetti and W. Weise, *Phys. Rev. D* **79**, 014022 (2009).
- [57] T. Hell, S. Rossner, M. Cristoforetti and W. Weise, *Phys. Rev. D* **81**, 074034 (2010).
- [58] K. Langfeld and C. Kettner, *Mod. Phys. Lett. A* **11**, 1331 (1996).
- [59] K. Langfeld, C. Kettner and H. Reinhardt, *Nucl. Phys. A* **608**, 331 (1996).
- [60] P. N. Meisinger and M. C. Ogilvie, *Phys. Lett. B* **379**, 163 (1996).
- [61] K. Fukushima, *Phys. Lett. B* **591**, 277 (2004).
- [62] K. I. Kondo, *Phys. Rev. D* **82**, 065024 (2010).
- [63] Y. Sakai, T. Sasaki, H. Kouno and M. Yahiro, *Phys. Rev. D* **82**, 076003 (2010).
- [64] D. Nickel and M. Buballa, *Phys. Rev. D* **79**, 054009 (2009).
- [65] S. Carignano, D. Nickel and M. Buballa, *Phys. Rev. D* **82**, 054009 (2010).
- [66] H. Abuki, D. Ishibashi and K. Suzuki, *Phys. Rev. D* **85**, 074002 (2012).
- [67] H. Abuki, *Phys. Lett. B* **728**, 427 (2014).
- [68] M. Frasca, arXiv:1602.04654 [hep-ph].
- [69] Z. F. Cui, I. C. Cloet, Y. Lu, C. D. Roberts, S. M. Schmidt, S. S. Xu and H. S. Zong, arXiv:1604.08454 [nucl-th].